Quaternion-Valued Multi-User MIMO Transmission via Dual-Polarized Antennas and QLLL Reduction

Sebastian Stern and Robert F.H. Fischer
Institute of Communications Engineering, Ulm University, Ulm, Germany
Email: {sebastian.stern, robert.fischer}@uni-ulm.de

***Abstract*—In this paper, quaternion-valued multi-user MIMO equalization is studied for the case of dual-polarized antennas. Given the multi-user MIMO uplink scenario, the relationship or transition between quaternion-valued arithmetic in transmitter/receiver processing and both vertically- and horizontally-polarized electromagnetic waves is discussed. A quaternion-valued system and channel model as well as related signal constellations are presented. Both linear and lattice-reduction-aided linear equalization are extended to the problem in hand. For that purpose, a quaternion-valued variant of the famous LLL lattice-reduction algorithm is proposed, which we call QLLL. Its gains in transmission performance and computational complexity over real- and complex-valued LLL reduction are discussed. Besides, the respective diversity orders are generalized to cope with the quaternion-valued channel model. The theoretical studies are complemented by results obtained from numerical simulations.**

I. Introduction

In wireless communications, multiple-input/multiple-output (MIMO) systems have enabled a large increase in data rates and reliability in comparison to classical single-input/single-output (SISO) transmission. Over the last decade, the focus has especially been on multi-user MIMO communication, i.e., handling the interference of several users that transmit at the same time at the same frequency. For that purpose, *lattice-reduction-aided* (LRA) equalization [19], [17] is a very powerful concept, exploiting the MIMO channel's diversity. However, as this approach has extensively been studied in the literature, cf., e.g., [16], [5], [14], the potential for further increases in performance is limited. For the upcoming communication systems (e.g., 5G), new strategies have to be found.

One promising strategy is the use of *dual-polarized antennas*, which have recently been presented [3], [9]. Particularly, (pairs of) antennas transmit or receive vertically and horizontally polarized electromagnetic waves simultaneously. Thereby, each polarization may be split into in-phase and quadrature component, altogether leading to *four* orthogonal basis functions, significantly increasing the spectral efficiency.

In the literature, it is well-known that the mathematical structure of *quaternions* is suited to describe a transmission in case of dual-polarized antennas [8], [18]. Based on that principle, *quaternion-valued* (QV) space-time codes and their maximum-likelihood decoding have been considered, e.g., in [13]. Besides, quaternions have been used to describe complex-valued (CV) eigenvalue distributions of multi-user MIMO channels [11]. Adaptive beamforming strategies for QV transmission have been proposed [10], however, implemented via equivalent real-valued (RV) matrix operations. Nevertheless, *low-complexity* equalization schemes for multi-user MIMO transmission that *directly employ QV arithmetic* are not available in the literature so far.

In this paper, we show how QV multi-user MIMO equalization may be performed. To this end, we exemplarily consider the uplink scenario, i.e., the *MIMO multiple-access channel*. We define a suited transition between QV arithmetic and CV transmission via dual-polarized antennas. Moreover, the construction of QV signal constellations is presented. The concepts of linear equalization (LE) and lattice-reduction-aided linear equalization (LRA LE) are extended to QV channels, including a discussion on the achievable diversity orders. For the latter, we propose a QV variant of the LLL algorithm [12], [16], [7], called *QLLL algorithm*. All theoretical derivations are assessed by Monte-Carlo simulations.

The paper is organized as follows: In Sec. II, mathematical properties of quaternions and related structures are reviewed. A QV system and channel model is given in Sec. III; the respective equalization strategies are proposed in Sec. IV. Numerical results w.r.t. performance and complexity are provided in Sec. V. The paper is summarized and concluded in Sec. VI.

II. Preliminaries

In the following, we briefly review the most important properties of quaternions and related lattices, cf., e.g., [2], [18].

A. Quaternions

The set of quaternions is defined as

$$\mathbb{H} = \{u = u^{(1)} + u^{(2)}\mathrm{i} + u^{(3)}\mathrm{j} + u^{(4)}\mathrm{k} \mid u^{(\chi)} \in \mathbb{R}\}\,, \quad (1)$$

where $u^{(\chi)}$, $\chi = 1, 2, 3, 4$, are RV components and $\mathrm{i}, \mathrm{j}, \mathrm{k}$ are *quaternion units*. The Hamilton equations [2] describe the relations between these units; they are represented in Table I.

Addition (and subtraction) of two quaternions u and v are performed componentwisely. The multiplication is defined by

$$\begin{aligned} u \cdot v = {} & (u^{(1)}v^{(1)} - u^{(2)}v^{(2)} - u^{(3)}v^{(3)} - u^{(4)}v^{(4)}) \\ & + (u^{(1)}v^{(2)} + u^{(2)}v^{(1)} + u^{(3)}v^{(4)} - u^{(4)}v^{(3)})\,\mathrm{i} \\ & + (u^{(1)}v^{(3)} - u^{(2)}v^{(4)} + u^{(3)}v^{(1)} + u^{(4)}v^{(2)})\,\mathrm{j} \\ & + (u^{(1)}v^{(4)} + u^{(2)}v^{(3)} - u^{(3)}v^{(2)} + u^{(4)}v^{(1)})\,\mathrm{k}\,. \end{aligned} \quad (2)$$

In Table I we can see the *non-commutativity* of the multiplication over $\mathbb{H}$, i.e., $u \cdot v \neq v \cdot u$ has to be kept in mind.

This work has been supported by Deutsche Forschungsgemeinschaft (DFG) under grant Fi 982/13-1.

TABLE I
HAMILTON EQUATIONS FOR $u \cdot v$, WHERE $u, v \in \{\mathrm{i}, \mathrm{j}, \mathrm{k}\}$.

u \ v	i	j	k
i	-1	$+\mathrm{k}$	$-\mathrm{j}$
j	$-\mathrm{k}$	-1	$+\mathrm{i}$
k	$+\mathrm{j}$	$-\mathrm{i}$	-1

The conjugate of u reads $u^* = u^{(1)} - u^{(2)}\mathrm{i} - u^{(3)}\mathrm{j} - u^{(4)}\mathrm{k}$ and its (Euclidean) norm is given by $\|u\| = \sqrt{uu^*} = \sqrt{u^*u} = \sqrt{(u^{(1)})^2 + (u^{(2)})^2 + (u^{(3)})^2 + (u^{(4)})^2}$. The inverse element (w.r.t. multiplication) has to be calculated via $u^{-1} = u^*/\|u\|^2$ to fulfill $uu^{-1} = 1$ (right inverse) and $u^{-1}u = 1$ (left inverse). Real part and imaginary part are defined by $\mathrm{Re}\{u\} = u^{(1)}$ and the tuple $\mathrm{Im}\{u\} = (u^{(2)}, u^{(3)}, u^{(4)})$, respectively.

The quaternions form an extension of the complex numbers $\mathbb{C}$, i.e., $\mathbb{H} = \mathbb{C} + \mathbb{C}\,\mathrm{j}$, where j is an "additional" imaginary unit. In particular, two complex numbers $\mu = \mu^{(1)} + \mu^{(2)}\,\mathrm{i}$ and $\nu = \nu^{(1)} + \nu^{(2)}\,\mathrm{i}$, where i is the imaginary unit of the complex numbers, are extended according to

$$\begin{aligned} u = \mu + \nu\,\mathrm{j} &= (\mu^{(1)} + \mu^{(2)}\mathrm{i}) + (\nu^{(1)} + \nu^{(2)}\mathrm{i})\,\mathrm{j} \\ &= \underbrace{\mu^{(1)}}_{u^{(1)}} + \underbrace{\mu^{(2)}}_{u^{(2)}}\,\mathrm{i} + \underbrace{\nu^{(1)}}_{u^{(3)}}\,\mathrm{j} + \underbrace{\nu^{(2)}}_{u^{(4)}}\,\underbrace{\mathrm{i}\cdot\mathrm{j}}_{\mathrm{k}} \,. \end{aligned} \tag{3}$$

Additionally, any quaternion $u = \mu + \nu\,\mathrm{j}$ can isomorphically be expressed via the 2×2 CV matrix

$$\boldsymbol{U}_{\mathrm{cv}} = \begin{bmatrix} \mu & -\nu \\ \nu^* & \mu^* \end{bmatrix} = \begin{bmatrix} u^{(1)} + u^{(2)}\,\mathrm{i} & -u^{(3)} - u^{(4)}\,\mathrm{i} \\ u^{(3)} - u^{(4)}\,\mathrm{i} & u^{(1)} - u^{(2)}\,\mathrm{i} \end{bmatrix} , \tag{4}$$

which translates (2) into a matrix representation.[1] It is a generalization of the real-valued description of a complex number [17], [7]. Following the same philosophy, we can represent any quaternion by the 4×4 RV matrix

$$\boldsymbol{U}_{\mathrm{rv}} = \begin{bmatrix} u^{(1)} & -u^{(2)} & -u^{(3)} & u^{(4)} \\ u^{(2)} & u^{(1)} & -u^{(4)} & -u^{(3)} \\ u^{(3)} & u^{(4)} & u^{(1)} & u^{(2)} \\ -u^{(4)} & u^{(3)} & -u^{(2)} & u^{(1)} \end{bmatrix} . \tag{5}$$

B. Lipschitz Integers

The *Lipschitz integers* (LIs) are defined by the set

$$\mathcal{L} = \{u = u^{(1)} + u^{(2)}\,\mathrm{i} + u^{(3)}\,\mathrm{j} + u^{(4)}\,\mathrm{k} \mid u^{(\chi)} \in \mathbb{Z}\} , \tag{6}$$

i.e., as all quaternions with only integer coefficients. They are isomorphic to the lattice $\mathbb{Z}^4$ and form a subring of $\mathbb{H}$ by analogy with the Gaussian integers $\mathcal{G} = \mathbb{Z} + \mathbb{Z}\,\mathrm{i}$ and $\mathbb{C}$.

The number of nearest neighbors is $\kappa_{\mathcal{L}} = 8$ [1], and the minimum squared distance between two elements reads $d^2_{\mathcal{L},\min} = 1$. The Voronoi region of $\mathcal{L}$ is a four-dimensional hypercube with 16 vertices, 32 edges, and 24 faces. For any quaternion $u \in \mathbb{H}$, the quantization to $\mathcal{L}$ is performed via

$$\mathcal{Q}_{\mathcal{L}}\{u\} = \lfloor u^{(1)} \rceil + \lfloor u^{(2)} \rceil\,\mathrm{i} + \lfloor u^{(3)} \rceil\,\mathrm{j} + \lfloor u^{(4)} \rceil\,\mathrm{k} , \tag{7}$$

[1]Noteworthy, (4) is not a unique way to represent (2). Other variants can be found in literature, e.g., in [11], with ν and $-\nu^*$ on the counterdiagonal.

Algorithm 1 Quantization to Hurwitz integers $\hat{u} = \mathcal{Q}_{\mathcal{H}}\{u\}$.

$\hat{u} = \mathrm{QUANT\_HURWITZ}(u)$

$u_{\mathrm{q}} = \lfloor u^{(1)} \rceil + \lfloor u^{(2)} \rceil\,\mathrm{i} + \lfloor u^{(3)} \rceil\,\mathrm{j} + \lfloor u^{(4)} \rceil\,\mathrm{k}$ ▷ $\mathcal{Q}_{\mathcal{L}}\{u\}$

$\widetilde{u}_{\mathrm{q}} = \lfloor u^{(1)} - 1/2 \rceil + \lfloor u^{(2)} - 1/2 \rceil\,\mathrm{i} + \lfloor u^{(3)} - 1/2 \rceil\,\mathrm{j} + \lfloor u^{(4)} - 1/2 \rceil\,\mathrm{k} + (1 + \mathrm{i} + \mathrm{j} + \mathrm{k})/2$ ▷ $\mathcal{Q}_{\mathcal{L}}\{u - \epsilon_{\mathcal{H}}\} + \epsilon_{\mathcal{H}}$

if $\|u - u_{\mathrm{q}}\| \leq \|u - \widetilde{u}_{\mathrm{q}}\|$ **then** ▷ Decide for closer point

  $\hat{u} = u_{\mathrm{q}}$ ▷ $\hat{u} \in \mathcal{L}$

else

  $\hat{u} = \widetilde{u}_{\mathrm{q}}$ ▷ $\hat{u} \in \mathcal{L} + \epsilon_{\mathcal{H}}$

end if

where $\lfloor \cdot \rceil$ denotes rounding w.r.t. $\mathbb{Z}$ (ties: rounding towards $+\infty$). The maximum squared quantization error is $e^2_{\mathcal{L},\max} = 1$ and occurs if $u \in \mathcal{L} + (1 + \mathrm{i} + \mathrm{j} + \mathrm{k})/2$.

Unfortunately, the LIs do not form a *Euclidean ring* [2]. Specifically, for $u, v, \sigma, \rho \in \mathcal{L}$, the right division with remainder $u = \sigma \cdot v + \rho$ is not a *Euclidean division* (aka division with *small* remainder) since for the case when $uv^{-1} \in \mathcal{L} + (1 + \mathrm{i} + \mathrm{j} + \mathrm{k})/2$, only the equality $\|\rho\| = \|v\|$ is achieved.

C. Hurwitz Integers

The non-Euclidean property of the LIs can be avoided by considering the ring of *Hurwitz integers* (HIs)

$$\begin{aligned} \mathcal{H} = \{u = u^{(1)} + u^{(2)}\,\mathrm{i} + u^{(3)}\,\mathrm{j} + u^{(4)}\,\mathrm{k} \mid \\ (u^{(1)}, u^{(2)}, u^{(3)}, u^{(4)}) \in \mathbb{Z}^4 \cup (\mathbb{Z} + 1/2)^4\} . \end{aligned} \tag{8}$$

It contains all LIs, i.e., $\mathcal{L} \subset \mathcal{H}$, and the set of LIs shifted by $\epsilon_{\mathcal{H}} = (1 + \mathrm{i} + \mathrm{j} + \mathrm{k})/2$. The additional elements ensure that the HIs form a Euclidean ring; thus a division with small remainder is ensured [2]. Nevertheless, $d^2_{\mathcal{H},\min} = 1$ remains: if balls with radius $r_{\mathrm{b}} = 1/2$ are centered at all LIs, there's still enough space to center additional balls at the points $\mathcal{L} + \epsilon_{\mathcal{H}}$ [2]. The nearest neighbors are tripled to $\kappa_{\mathcal{H}} = 24$, though. The HIs are isomorphic to the *checkerboard* or *Schläfli lattice* $\boldsymbol{D}_4$, which has the densest packing in four dimensions [1].

The Voronoi region of $\mathcal{H}$ is a four-dimensional 24-cell with 24 vertices, 96 edges, and 96 faces [2]. A low-complexity quantization w.r.t. $\mathcal{H}$ is, however, still possible and realized in Algorithm 1. The maximum squared quantization error is $e^2_{\mathcal{H},\max} = 0.5$ and occurs, e.g., if $u = 0.5 + 0.5\,\mathrm{i}$.

III. System and Channel Model

Subsequently, we present a system and channel model for QV multi-user MIMO uplink transmission.

A. Quaternion-Valued System Model

We are interested in a QV multi-user MIMO transmission over the MIMO multiple-access channel, where K non-cooperating transmitters (TXs) communicate to a joint receiver (RX). The related discrete-time baseband model is depicted in Fig. 1 and described by the QV system equation

$$\boldsymbol{y} = \boldsymbol{H}\boldsymbol{x} + \boldsymbol{n} . \tag{9}$$

In each time step, the K users radiate QV symbols, in vector notation $\boldsymbol{x} = [x_1, \ldots, x_K]^{\mathsf{T}} \in \mathbb{H}^K$. They are drawn from a constellation $\mathcal{A}$ forming a subset of $\mathbb{H}$, i.e., $\boldsymbol{x} \in \mathcal{A}^K \subset \mathbb{H}^K$. Its

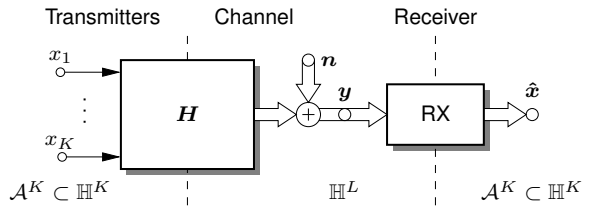

Fig. 1. System model for quaternion-valued multi-user MIMO transmission.

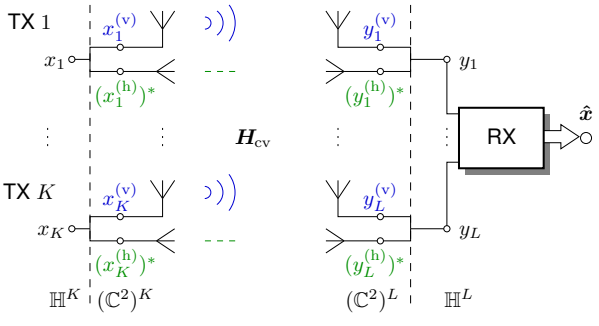

Fig. 2. Quaternion-valued multi-user MIMO transmission via pairs of polarized antennas (vertical polarization: blue; horizontal polarization: green), each antenna radiating/receiving a complex-valued symbol (baseband notation).

cardinality reads $M = |\mathcal{A}|$. The MIMO channel is represented by the QV matrix

$$\boldsymbol{H} = \big[h_{l,k}\big]_{\substack{l=1,\dots,L\\k=1,\dots,K}} \in \mathbb{H}^{L\times K} \,. \tag{10}$$

The vector $\boldsymbol{n} = [n_1, \dots, n_L]^{\mathsf{T}} \in \mathbb{H}^L$ represents additive QV noise that is present at the $L \geq K$ receiving units. They provide the QV receive symbols $\boldsymbol{y} = [y_1, \dots, y_L]^{\mathsf{T}} \in \mathbb{H}^L$. After joint processing, we obtain the vector of estimated QV symbols $\hat{\boldsymbol{x}} = [\hat{x}_1, \dots, \hat{x}_K]^{\mathsf{T}} \in \mathcal{A}^K$.

B. Equivalent Complex-Valued Dual-Polarized System Model

QV symbols are well-suited to model a CV transmission via pairs of polarized (aka *dual-polarized*) antennas as illustrated in Fig. 2 and originally described for the SISO case [8], [18].

To this end, we take advantage of the CV representation of a quaternion (4). The equivalent system equation of (9) reads

$$\underbrace{\begin{bmatrix}\boldsymbol{y}^{(\mathrm{v})}\\(\boldsymbol{y}^{(\mathrm{h})})^*\end{bmatrix}}_{\boldsymbol{y}_{\mathrm{cv}}} = \underbrace{\begin{bmatrix}\boldsymbol{H}^{(\mathrm{d})} & -\boldsymbol{H}^{(\mathrm{c})}\\(\boldsymbol{H}^{(\mathrm{c})})^* & (\boldsymbol{H}^{(\mathrm{d})})^*\end{bmatrix}}_{\boldsymbol{H}_{\mathrm{cv}}} \underbrace{\begin{bmatrix}\boldsymbol{x}^{(\mathrm{v})}\\(\boldsymbol{x}^{(\mathrm{h})})^*\end{bmatrix}}_{\boldsymbol{x}_{\mathrm{cv}}} + \underbrace{\begin{bmatrix}\boldsymbol{n}^{(\mathrm{v})}\\(\boldsymbol{n}^{(\mathrm{h})})^*\end{bmatrix}}_{\boldsymbol{n}_{\mathrm{cv}}} \,. \tag{11}$$

We have the CV transmit vectors $\boldsymbol{x}^{(\mathrm{v})} = \boldsymbol{x}^{(1)} + \boldsymbol{x}^{(2)}\mathrm{i}$ and $(\boldsymbol{x}^{(\mathrm{h})})^* = \boldsymbol{x}^{(3)} - \boldsymbol{x}^{(4)}\mathrm{i}$, the noise vectors $\boldsymbol{n}^{(\mathrm{v})} = \boldsymbol{n}^{(1)} + \boldsymbol{n}^{(2)}\mathrm{i}$ and $(\boldsymbol{n}^{(\mathrm{h})})^* = \boldsymbol{n}^{(3)} - \boldsymbol{n}^{(4)}\mathrm{i}$, as well as the receive vectors $\boldsymbol{y}^{(\mathrm{v})} = \boldsymbol{y}^{(1)} + \boldsymbol{y}^{(2)}\mathrm{i}$ and $(\boldsymbol{y}^{(\mathrm{h})})^* = \boldsymbol{y}^{(3)} - \boldsymbol{y}^{(4)}\mathrm{i}$. Besides, subchannels $\boldsymbol{H}^{(\mathrm{d})} = \boldsymbol{H}^{(1)} + \boldsymbol{H}^{(2)}\mathrm{i}$ and $(\boldsymbol{H}^{(\mathrm{c})})^* = \boldsymbol{H}^{(3)} - \boldsymbol{H}^{(4)}\mathrm{i}$ are present. Thereby, $\boldsymbol{x}^{(\chi)}$, $\boldsymbol{H}^{(\chi)}$, $\boldsymbol{n}^{(\chi)}$, and $\boldsymbol{y}^{(\chi)}$ are the RV components of the QV variables $\boldsymbol{x}$, $\boldsymbol{H}$, $\boldsymbol{n}$, and $\boldsymbol{y}$.

In order to realize a transmission according to (11), in transmitter $k = 1, \dots, K$, the QV data symbols are split into

$$x_k = \underbrace{\big(x_k^{(1)} + x_k^{(2)}\mathrm{i}\big)}_{x_k^{(\mathrm{v})}} + \underbrace{\big(x_k^{(3)} - x_k^{(4)}\mathrm{i}\big)^*}_{(x_k^{(\mathrm{h})})^*}\mathrm{j} \,. \tag{12}$$

Then, after modulation to radio frequency, the first CV part $x_k^{(\mathrm{v})}$ is radiated from an antenna where the electromagnetic waves possess a *vertical* polarization. In contrast, the second part $(x_k^{(\mathrm{h})})^*$ is radiated via *horizontally* polarized waves from another antenna, achieving orthogonality between them.

When considering pairs of polarized transmit/receive antennas with index k and l and neglecting interference from other transmitters (single-user point-to-point scenario), the QV transmission (9) equivalently reads

$$\begin{bmatrix}\tilde{y}_l^{(\mathrm{v})}\\(\tilde{y}_l^{(\mathrm{h})})^*\end{bmatrix} = \begin{bmatrix}h_{l,k}^{(\mathrm{d})} & -h_{l,k}^{(\mathrm{c})}\\(h_{l,k}^{(\mathrm{c})})^* & (h_{l,k}^{(\mathrm{d})})^*\end{bmatrix}\begin{bmatrix}x_k^{(\mathrm{v})}\\(x_k^{(\mathrm{h})})^*\end{bmatrix} + \begin{bmatrix}n_l^{(\mathrm{v})}\\(n_l^{(\mathrm{h})})^*\end{bmatrix} \,. \tag{13}$$

Thereby, $h_{l,k}^{(\mathrm{d})}$ describes the CV gain for the *direct* links between identically polarized antennas, and $(h_{l,k}^{(\mathrm{c})})^*$ the *cross* links to the antennas which are differently polarized.[2] Combining both into one quaternion, we obtain

$$h_{l,k} = \underbrace{\big(h_{l,k}^{(1)} + h_{l,k}^{(2)}\mathrm{i}\big)}_{\text{direct link } h_{l,k}^{(\mathrm{d})}} + \underbrace{\big(h_{l,k}^{(3)} - h_{l,k}^{(4)}\mathrm{i}\big)^*}_{\text{cross link } (h_{l,k}^{(\mathrm{c})})^*}\mathrm{j} \,. \tag{14}$$

At the receiver side, each of the $L \geq K$ units has one receive antenna for vertical and one for horizontal polarization, i.e., for $l = 1, \dots, L$, we obtain the symbols

$$y_l = \underbrace{\big(y_l^{(1)} + y_l^{(2)}\mathrm{i}\big)}_{y_l^{(\mathrm{v})}} + \underbrace{\big(y_l^{(3)} - y_l^{(4)}\mathrm{i}\big)^*}_{(y_l^{(\mathrm{h})})^*}\mathrm{j} \,. \tag{15}$$

Besides, we have to deal with QV additive noise

$$n_l = \underbrace{\big(n_l^{(1)} + n_l^{(2)}\mathrm{i}\big)}_{n_l^{(\mathrm{v})}} + \underbrace{\big(n_l^{(3)} - n_l^{(4)}\mathrm{i}\big)^*}_{(n_l^{(\mathrm{h})})^*}\mathrm{j} \,, \tag{16}$$

representing the combined noise from both polarized antennas.

C. Channel Model

Throughout the paper, we assume a QV flat-fading model [18], where the channel matrix is assumed to be constant over a block of symbols (*block-fading channel*).

The i.i.d. channel coefficients in (10) consist of four i.i.d. zero-mean RV Gaussian random variables with variance $\sigma_h^2/4 = 1/4$, or in an alternative point of view, two independent CV random variables $h_{l,k}^{(\mathrm{d})}$ and $h_{l,k}^{(\mathrm{c})}$ with variance $\sigma_h^2/2 = 1/2$, cf. (14). Thereby, $h_{l,k}^{(\mathrm{d})}$ represents fading for the direct links, and $h_{l,k}^{(\mathrm{c})}$ cross-polar scattering [18]. Given the point-to-point scenario (13), both CV receive symbols $\tilde{y}_{l,k}^{(\mathrm{v})}$ and $\big(\tilde{y}_{l,k}^{(\mathrm{h})}\big)^*$ consequently possess a Rayleigh distribution.

The QV noise samples n_l in (16) are assumed to be i.i.d. and white over time and consist of four i.i.d. zero-mean RV Gaussian components with variance $\sigma_n^2/4$. Since two antennas are required for each QV symbol, $\sigma_n^2 = 2\,\sigma_{n,\mathrm{cv}}^2$, where $\sigma_{n,\mathrm{cv}}^2$ is the CV noise variance. Defining the signal-to-noise ratio

[2] We see from (13) that a QV representation of a 2×2 CV MIMO channel is possible if certain dependencies between the channel gains are present. In particular, these dependencies occur if the polarization planes and quadrature up-/down-mixing are kept orthogonal at both TX and RX [18].

(SNR) as transmitted energy per bit $E_{\mathrm{b,TX}}$ over the noise power spectral density N_0 and denoting $\sigma_{a,\mathrm{cv}}^2$ and M_{cv} as the constellation's variance and cardinality in case of CV systems,

$$\frac{E_{\mathrm{b,TX}}}{N_0} = \frac{\sigma_{a,\mathrm{cv}}^2}{\sigma_{n,\mathrm{cv}}^2 \log_2(M_{\mathrm{cv}})} = 2 \cdot \frac{\sigma_a^2}{\sigma_n^2 \log_2(M)} \,. \tag{17}$$

D. Signal Constellation

We subsequently consider how the signal constellation $\mathcal{A}$ can be chosen in case of QV data symbols.

1) Constellations over Lipschitz Integers: We extend the philosophy of square QAM to four dimensions. Demanding the minimum squared distance $d_{\min}^2 = 1$, we choose

$$\mathcal{A}_{\mathcal{L}} = \mathcal{A}_{\mathrm{d}} + \mathcal{A}_{\mathrm{d}}\,\mathrm{i} + \mathcal{A}_{\mathrm{d}}\,\mathrm{j} + \mathcal{A}_{\mathrm{d}}\,\mathrm{k} \,, \tag{18}$$

with the zero-mean RV components

$$\mathcal{A}_{\mathrm{d}} = \big\{ m - (M_{\mathrm{d}} - 1)/2 \mid m \in \{0, \ldots, M_{\mathrm{d}} - 1\} \big\} \,. \tag{19}$$

Thereby, $M_{\mathrm{d}} = 2^{\psi}$, $\psi \in \mathbb{N}$, denotes the cardinality in each RV dimension, i.e., the total cardinality reads $M = M_{\mathrm{d}}^4 = 16, 256, 4096, \ldots$ We are able to map $R_{\mathrm{m}} = \log_2(M) = 4\,\psi$ bits directly to the constellation points by extending the strategy of Gray labeling to four dimensions. The data symbols' variance reads $\sigma_{x,\mathcal{L}}^2 = (M_{\mathrm{d}}^2 - 1)/3 = (\sqrt{M} - 1)/3$, i.e., it is doubled in comparison to a square QAM constellation $\mathcal{A}_{\mathcal{G}} = \mathcal{A}_{\mathrm{d}} + \mathcal{A}_{\mathrm{d}}\,\mathrm{i}$ with the same M_{d}. Coincidentally, the number of transmitted bits per symbols is doubled. Noteworthy, in order to enable the zero-mean property in (18), $\mathcal{A}_{\mathcal{L}} \subset \mathcal{L} + o_{\mathcal{L}}$, i.e., the offset $o_{\mathcal{L}} = (1+\mathrm{i}+\mathrm{j}+\mathrm{k})/2$ to the LI lattice is present.

2) Constellations over Hurwitz Integers: Taking advantage of the HIs, we are able to construct constellations that are more densely packed—preserving the same minimum squared distance $d_{\min}^2 = 1$ (cf. Sec. II-C). Following (8), a zero-mean HI-based constellation is composed of

$$\mathcal{A}_{\mathcal{H}} = \mathcal{A}_{\mathcal{L},1} \cup \mathcal{A}_{\mathcal{L},2} \,, \tag{20}$$

i.e., two shifted LI-based constellations (partitions)

$$\mathcal{A}_{\mathcal{L},1} = \mathcal{A}_{\mathcal{L}} - (1 + \mathrm{i} + \mathrm{j} + \mathrm{k})/4 \tag{21}$$

$$\mathcal{A}_{\mathcal{L},2} = \mathcal{A}_{\mathcal{L}} + (1 + \mathrm{i} + \mathrm{j} + \mathrm{k})/4 \,, \tag{22}$$

with mutual distance $\epsilon_{\mathcal{H}} = (1 + \mathrm{i} + \mathrm{j} + \mathrm{k})/2$, as illustrated in Fig. 3. Choosing $M_{\mathrm{d}} = 2^{\psi}$ signal points per dimension for each set, we hence obtain the cardinalities $M = 2\,M_{\mathrm{d}}^4 = 32, 512, 8192, \ldots$ The data symbols' variance now reads $\sigma_{x,\mathcal{H}}^2 = (M_{\mathrm{d}}^2 - 1)/3 + 0.25 = (\sqrt{M/2} - 1)/3 + 0.25$, i.e., independently from M_{d} or M the doubled cardinality is achieved with only a very small increase in power.[3] It is worth mentioning that $\mathcal{A}_{\mathcal{H}} \subset \mathcal{H} + o_{\mathcal{H}}$, where the offset $o_{\mathcal{H}} = (1 + \mathrm{i} + \mathrm{j} + \mathrm{k})/4$ to the HI lattice is present.

For these constellations, a Gray labeling is not possible ($\kappa_{\mathcal{H}} = 24$ vs. $\kappa_{\mathcal{L}} = 8$; cf. Sec. II-C). Nevertheless, we can employ the strategy depicted in Fig. 3: The leftmost bit controls which partition is chosen; the remaining bits determine the signal point within the selected partition $\mathcal{A}_{\mathcal{L},1}$ or $\mathcal{A}_{\mathcal{L},2}$. Thereby, a Gray labeling is applied for each subset.

[3] $\mathcal{A}_{\mathcal{H}}$ with cardinality M has the same variance as its $M/2$-ary partitions $\mathcal{A}_{\mathcal{L},1}$, $\mathcal{A}_{\mathcal{L},2}$ plus an offset-related increase of $4 \cdot 0.25^2 = 0.25$.

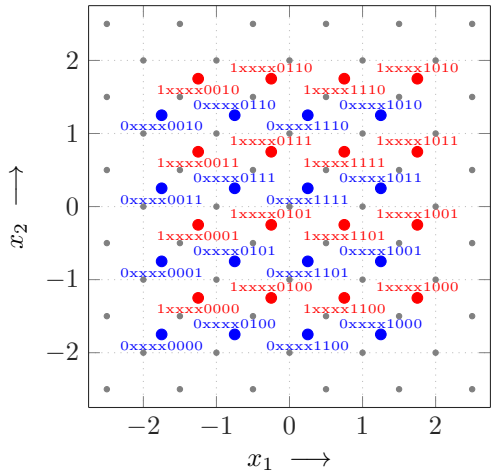

Fig. 3. Projection onto the first two components x_1 and x_2 of a 512-ary zero-mean HI-based constellation $\mathcal{A}_{\mathcal{H}}$ (blue and red points represent partitions $\mathcal{A}_{\mathcal{L},1}$ and $\mathcal{A}_{\mathcal{L},2}$, respectively). The projection of the HIs (gray; without offset) and a suited bit labeling are additionally shown.

IV. Quaternion-Valued Multi-User MIMO Equalization and the QLLL Algorithm

Given the above QV multi-user MIMO system and channel model, we now discuss how the receiver/equalization part in Fig. 1 may be implemented.

A. Linear Equalization

A simple way to handle the multi-user interference is the LE via $\tilde{\boldsymbol{y}} = \boldsymbol{F}\boldsymbol{y}$, where $\boldsymbol{F} \in \mathbb{H}^{K \times L}$ is—for the channel model in hand—a QV equalization matrix. For LE according to the minimum mean-square error (MMSE) criterion, we consider

$$\bar{\boldsymbol{F}} = \bar{\boldsymbol{H}}^{+} = (\bar{\boldsymbol{H}}^{\mathsf{H}} \bar{\boldsymbol{H}})^{-1} \bar{\boldsymbol{H}}^{\mathsf{H}} \,, \qquad \bar{\boldsymbol{H}} = \begin{bmatrix} \boldsymbol{H} \\ \sqrt{\zeta}\boldsymbol{I} \end{bmatrix} \,, \tag{23}$$

where $\bar{\boldsymbol{H}} \in \mathbb{H}^{(L+K) \times K}$ is the *augmented channel matrix* with inverse TX-side SNR $\zeta = \sigma_n^2/\sigma_x^2$ and $\bar{\boldsymbol{F}} \in \mathbb{H}^{K \times (L+K)}$ is its left pseudo-inverse[4] called *augmented equalization matrix*, cf., e.g., [4]. Then, $\boldsymbol{F}$ is given by the $K \times L$ left part of $\bar{\boldsymbol{F}}$.

After equalization, the noisy symbols $\tilde{\boldsymbol{y}}$ are decoded to obtain estimates $\hat{\boldsymbol{x}} = \mathrm{DEC}\{\tilde{\boldsymbol{y}}\} \in \mathcal{A}^K$. The performance (or the achievable rate in the coded case) is determined by the row norms of $\bar{\boldsymbol{F}} = [\bar{\boldsymbol{f}}_1^{\mathsf{H}}, \ldots \bar{\boldsymbol{f}}_K^{\mathsf{H}}]^{\mathsf{H}}$, which yield the K noise powers $\tilde{\sigma}_{n,k}^2 = \sigma_n^2 \|\bar{\boldsymbol{f}}_k^{\mathsf{H}}\|^2$ at the input of the decoders.[5]

In the CV case, LE achieves the well-known diversity order[6] $\Delta_{\mathrm{LE,cv}} = L - K + 1$, i.e., $\Delta_{\mathrm{LE,cv}} = 1$ for $K = L$. However, considering the QV channel (10), each coefficient possesses *four* RV Gaussian random variables instead of *two*, i.e., *the diversity of the MIMO channel is doubled*. Denoting D_{ch} as the

[4] The Hermitian $\boldsymbol{A}^{\mathsf{H}}$ of a QV matrix $\boldsymbol{A}$ is its conjugated transpose (cf. Sec. II). The inverse matrix $\boldsymbol{A}^{-1}$ may, e.g., be obtained via the Gauss-Jordan procedure, taking non-commutative multiplications into account.

[5] It is worth mentioning that, using the CV or RV isomorphic representations (4) or (5), we are able to equalize the QV system via CV/RV matrices. However, due to isomorphic calculations, all variants yield the same performance.

[6] Diversity order Δ means that the error curve asymptotically decays Δ decades for an increase in SNR of 10 dB, i.e., Δ describes the error curve's slope on a double-logarithmic scale.

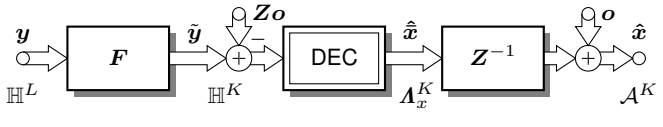

Fig. 4. Receiver model of quaternion-valued lattice-reduction-aided equalization for the K-user MIMO multiple-access channel.

number of components (*dimension*) per channel coefficient—$D_{\mathrm{ch}} = 1$ for RV, $D_{\mathrm{ch}} = 2$ for CV, and $D_{\mathrm{ch}} = 4$ for QV channels—we can generalize the diversity order of LE to[7]

$$\Delta_{\mathrm{LE}} = D_{\mathrm{ch}}/2 \cdot (L - K + 1) \, . \tag{24}$$

Hence, if $K = L$, we obtain diversity order "one half" for RV channels [15], one for CV channels, and two for QV channels.

B. Lattice-Reduction-Aided Linear Equalization

To overcome the abovementioned diversity limitation of LE, LRA LE has been proposed [19], [17]. In the following, we discuss how LRA LE can be performed in the case of QV transmission.

1) Receiver Model: In MMSE LRA LE, the augmented equalization matrix is obtained via [5]

$$\underbrace{\bar{\boldsymbol{F}}^{\mathsf{H}}}_{\boldsymbol{G}_{\mathrm{red}}} = \underbrace{(\bar{\boldsymbol{H}}^{+})^{\mathsf{H}}}_{\boldsymbol{G}} \underbrace{\boldsymbol{Z}^{\mathsf{H}}}_{\boldsymbol{T}} \, . \tag{25}$$

To this end, the Hermitian of $\bar{\boldsymbol{H}}^{+}$ from (23) is interpreted as the generator matrix $\boldsymbol{G} = (\bar{\boldsymbol{H}}^{+})^{\mathsf{H}}$ of a lattice, and the *full-rank integer matrix* $\boldsymbol{T} = \boldsymbol{Z}^{\mathsf{H}} \in \boldsymbol{\Lambda}_x^{K \times K}$ describes a change of basis [5], [14]. Choosing $\boldsymbol{Z}$ conveniently, the row norms of $\boldsymbol{G}_{\mathrm{red}}^{\mathsf{H}} = \bar{\boldsymbol{F}}$ are lowered in comparison to LE (23), in turn leading to an increased performance. The elements of $\boldsymbol{Z}$ are taken from the signal-point lattice $\boldsymbol{\Lambda}_x$ (the lattice the data symbols are drawn from neglecting an offset). For the QV constellations (18) or (20) this means $\boldsymbol{\Lambda}_x = \mathcal{L}$ or $\boldsymbol{\Lambda}_x = \mathcal{H}$.

The QV LRA receiver is depicted in Fig. 4. First, the noisy receive symbols are linearly equalized via the $K \times L$ left part of $\bar{\boldsymbol{F}}$ obtained from (25). Subsequently, the channel decoding is performed (DEC).[8] To that purpose, the offset induced by the signal constellation, particularly given by $\boldsymbol{Zo} = \boldsymbol{Z}\,[o, \ldots, o]^{\mathsf{T}}$ with $o = o_{\mathcal{L}}$ or $o = o_{\mathcal{H}}$, has to be removed to obtain valid lattice points, cf., e.g., [17]. Then, the change of basis is reversed via $\boldsymbol{Z}^{-1}$. After adding the offset $\boldsymbol{o}$, we obtain the estimated symbols $\hat{x}_1, \ldots, \hat{x}_K \in \mathcal{A}$.

We still have to clarify how to choose $\boldsymbol{Z}$ conveniently. From the CV case ($\boldsymbol{\Lambda}_x = \mathcal{G}$), it is known that the *successive minima* of the lattice spanned by $\boldsymbol{G} = (\bar{\boldsymbol{H}}^{+})^{\mathsf{H}}$ optimally solve (25), cf., e.g., [5], [14]. For the situation in hand, the successive minima w.r.t. $\boldsymbol{\Lambda}_x = \mathcal{L}$ or $\boldsymbol{\Lambda}_x = \mathcal{H}$ are required. Unfortunately, their determination is an NP-hard problem, resulting in a huge computational effort. Instead, we consider how the polynomial-time Lenstra-Lenstra-Lovász (LLL) algorithm can be adapted to the QV case, approximately solving (25) by obtaining a unimodular integer matrix ($|\det(\boldsymbol{Z})| = 1$).

[7]Due to space limitations, formal proofs are omitted in this paper.

[8]In the uncoded case, we have a simple quantization w.r.t. $\boldsymbol{\Lambda}_x$. A coded transmission is, e.g., possible via multi-level codes, cf. [6].

2) LLL Reduction over Lipschitz Integers: The LLL algorithm can be interpreted as a generalization of the Euclidean algorithm [12]. It operates on the decomposition $\boldsymbol{G}_{\mathrm{red}} = \boldsymbol{QR}$, $\boldsymbol{Q} = [\boldsymbol{q}_1, \ldots, \boldsymbol{q}_K]$ an $L \times K$ matrix with orthogonal columns and $\boldsymbol{R} = [r_{l,k}]$ a $K \times K$ upper triangular matrix with unit main diagonal. It has originally been defined for the RV case (RLLL; $\boldsymbol{\Lambda}_x = \mathbb{Z}$), forcing the *size-reduction condition*

$$|r_{l,k}| \leq 1/2 \quad \widehat{=} \quad \mathcal{Q}_{\mathbb{Z}}\{r_{l,k}\} = 0 \, , \quad 1 \leq l < k \leq K \, , \tag{26}$$

followed by the *Lovász condition* (swapping condition)

$$\|\boldsymbol{q}_k\|^2 \geq (\delta - \|r_{k-1,k}\|^2)\|\boldsymbol{q}_{k-1}\|^2 \, , \quad k = 2, \ldots, K \, . \tag{27}$$

The quality parameter δ controls the trade-off between strength of reduction and complexity. As the maximum squared quantization error of $\mathcal{Q}_{\mathbb{Z}}\{\cdot\} = \lfloor \cdot \rceil$ is $e^2_{\mathbb{Z},\max} = 1/4$ and hence $\|r_{k-1,k}\|^2 \leq 1/4$ after (26), we have to demand $\delta \in (1/4, 1]$ for (27). If $\delta \leq 1/4$, (27) may be fulfilled independently from $\boldsymbol{q}_k$ and $\boldsymbol{q}_{k-1}$, resulting in an inoperative reduction.

The RLLL has been extended to the CV case [7] (CLLL; $\boldsymbol{\Lambda}_x = \mathcal{G}$). Thereby, the Lovász condition (27) is kept unchanged, but the size reduction (26) is adapted to

$$|r^{(1)}_{l,k}| \leq 1/2 \cap |r^{(2)}_{l,k}| \leq 1/2 \quad \widehat{=} \quad \mathcal{Q}_{\mathcal{G}}\{r_{l,k}\} = 0 \, . \tag{28}$$

Since $e^2_{\mathcal{G},\max} = 2 \cdot (0.5)^2 = 1/2$ and hence $\|r_{k-1,k}\|^2 \leq 1/2$ after size reduction, we now have to demand $\delta \in (1/2, 1]$.

If the size reduction is extended to the LIs ($\boldsymbol{\Lambda}_x = \mathcal{L}$), the condition reads $\mathcal{Q}_{\mathcal{L}}\{r_{l,k}\} = 0$, cf. (7). We know from Sec. II that $e^2_{\mathcal{L},\max} = 1$, i.e., even if the maximum parameter $\delta = 1$ is chosen, (27) may become inoperative since $\|r_{k-1,k}\|^2 \leq 1$. Hence, *an LLL reduction over the LIs cannot be defined*,[9] which is a consequence of the non-Euclidean property of $\mathcal{L}$.

3) LLL Reduction over Hurwitz Integers: Considering the HIs ($\boldsymbol{\Lambda}_x = \mathcal{H}$), the size-reduction condition (26) reads

$$\mathcal{Q}_{\mathcal{H}}\{r_{l,k}\} = 0 \, , \quad 1 \leq l < k \leq K \, , \tag{29}$$

cf. Algorithm 1. We know that $e^2_{\mathcal{H},\max} = 1/2$, i.e., after size reduction, $\|r_{k-1,k}\|^2 \leq 1/2$ is valid. This allows us to use a parameter $\delta \in (1/2, 1]$ in (27). Since $\mathcal{H}$ is a Euclidean ring, the LLL reduction is properly defined.[10] Following the abbreviations RLLL and CLLL, we call this strategy and the related algorithm QLLL (Q for quaternions). Noteworthy, as $\mathcal{L} \subset \mathcal{H}$, the QLLL is also suited for LI-based constellations (18).

Obeying the rules of QV arithmetic, the QLLL can be realized by analogy with the CLLL [7] as implemented in Algorithm 2: First, $\boldsymbol{Q}$ and $\boldsymbol{R}$ are calculated via Gram-Schmidt orthogonalization (GSO) *with pivoting*; the pivoting speeds up the reduction [4] (Lines 3–13). Then, the reduction is performed (Lines 15–27). In SIZE_REDUCE, $\mathcal{Q}_{\mathcal{H}}\{\cdot\}$ is applied.

[9]In the case of QV channels and LI-based constellations (18), we are able to employ the RLLL to the $4L \times 4K$ RV representation (5) of $\boldsymbol{G} = (\boldsymbol{H}^{+})^{\mathsf{H}}$, or the CLLL to the $2L \times 2K$ CV one (4), respectively. Then, the QV system is decomposed into its RV/CV components and all operations are performed in RV/CV arithmetic, counteracting the idea of QV equalization.

[10]The LLL reduction for Euclidean rings like $\mathcal{G}$ or $\mathcal{H}$ has *mathematically* been discussed in [12] even before the CLLL was proposed. However, these considerations were restricted to the "standard" parameter $\delta = 0.75$, without giving the practically-relevant conditions (28) or (29) and related algorithms.

Algorithm 2 QLLL reduction of $\boldsymbol{G}$ with parameter $\delta \in (0.5, 1]$.

$[\boldsymbol{G}_{\mathrm{red}}, \boldsymbol{Q}, \boldsymbol{R}, \boldsymbol{T}] = \mathrm{QLLL}(\boldsymbol{G}, \delta)$ ▷ $\boldsymbol{G} = [\boldsymbol{g}_1, \ldots, \boldsymbol{g}_K]$

1: $\boldsymbol{G}_{\mathrm{red}} = \boldsymbol{G}$, $\boldsymbol{Q} = \boldsymbol{G}$, $\boldsymbol{R} = \boldsymbol{I}$, $\boldsymbol{T} = \boldsymbol{I}$, $k = 1$
2: $\boldsymbol{\omega} = [\|\boldsymbol{q}_1\|^2, \ldots, \|\boldsymbol{q}_K\|^2]$ ▷ $\boldsymbol{\omega} = [\omega_1, \ldots, \omega_K]$
3: **while** $k \leq K$ **do** ▷ GSO with pivoting
4: $\quad \widetilde{k} = \mathrm{argmin}_{m=k,\ldots,K}\, \omega_m$ ▷ pivoting
5: $\quad$ **if** $\widetilde{k} \neq k$ **then**
6: $\quad\quad$ move column $\widetilde{k}$ to position k in $\boldsymbol{G}_{\mathrm{red}}$, $\boldsymbol{Q}$, $\boldsymbol{R}$, $\boldsymbol{T}$, $\boldsymbol{\omega}$
7: $\quad$ **end if**
8: $\quad$ **for** $l = k+1, \ldots, K$ **do** ▷ orthogonal projection
9: $\quad\quad r_{k,l} = \boldsymbol{q}_k^{\mathsf{H}} \boldsymbol{q}_l / \omega_k$ ▷ k^{th} row and l^{th} column of $\boldsymbol{R}$
10: $\quad\quad \boldsymbol{q}_l = \boldsymbol{q}_l - \boldsymbol{q}_k\, r_{k,l}\,, \quad \omega_l = \omega_l - \omega_k \|\boldsymbol{r}_{k,l}\|^2$
11: $\quad$ **end for**
12: $\quad k = k + 1$ ▷ next step
13: **end while**
14: $k = 2$
15: **while** $k \leq K$ **do** ▷ QLLL reduction
16: $\quad [\boldsymbol{G}_{\mathrm{red}}, \boldsymbol{R}, \boldsymbol{T}] = \mathrm{SIZE\_REDUCE}(k-1, k, \boldsymbol{G}_{\mathrm{red}}, \boldsymbol{R}, \boldsymbol{T})$
17: $\quad$ **if** $\omega_k < (\delta - \|r_{k-1,k}\|^2)\, \omega_{k-1}$ **then** ▷ Lovász condition
18: $\quad\quad$ swap columns $k-1$ and k in $\boldsymbol{G}_{\mathrm{red}}$ and $\boldsymbol{T}$
19: $\quad\quad [\boldsymbol{Q}, \boldsymbol{R}, \boldsymbol{\omega}] = \mathrm{UPDATE\_QR}(\boldsymbol{Q}, \boldsymbol{R}, \boldsymbol{\omega}, k)$
20: $\quad\quad k = \max\{2, k-1\}$ ▷ back to step $k-1$
21: $\quad$ **else**
22: $\quad\quad$ **for** $l = k-2, k-3, \ldots, 1$ **do** ▷ residual size-reduction
23: $\quad\quad\quad [\boldsymbol{G}_{\mathrm{red}}, \boldsymbol{R}, \boldsymbol{T}] = \mathrm{SIZE\_REDUCE}(l, k, \boldsymbol{G}_{\mathrm{red}}, \boldsymbol{R}, \boldsymbol{T})$
24: $\quad\quad$ **end for**
25: $\quad\quad k = k + 1$ ▷ next step
26: $\quad$ **end if**
27: **end while**

$[\boldsymbol{G}_{\mathrm{red}}, \boldsymbol{R}, \boldsymbol{T}] = \mathrm{SIZE\_REDUCE}(l, k, \boldsymbol{G}_{\mathrm{red}}, \boldsymbol{R}, \boldsymbol{T})$

1: $\rho = \mathrm{QUANT\_HURWITZ}(r_{l,k})$ ▷ $\mathcal{Q}_{\mathcal{H}}\{\cdot\}$, cf. Algorithm 1
2: **if** $\rho > 0$ **then** ▷ already size-reduced if $\rho = 0$
3: $\quad \boldsymbol{g}_{\mathrm{red},k} = \boldsymbol{g}_{\mathrm{red},k} - \boldsymbol{g}_{\mathrm{red},l}\, \rho$
4: $\quad \boldsymbol{r}_{1:l,k} = \boldsymbol{r}_{1:l,k} - \boldsymbol{r}_{1:l,l}\, \rho$ ▷ upper l rows of $\boldsymbol{R}$
5: $\quad \boldsymbol{t}_k = \boldsymbol{t}_k - \boldsymbol{t}_l\, \rho$
6: **end if**

$[\boldsymbol{Q}, \boldsymbol{R}, \boldsymbol{\omega}] = \mathrm{UPDATE\_QR}(\boldsymbol{Q}, \boldsymbol{R}, \boldsymbol{\omega}, k)$ ▷ update GSO, cf. [7]

1: $\widetilde{\boldsymbol{q}}_{k-1} = \boldsymbol{q}_{k-1}$, $\widetilde{\boldsymbol{R}} = \boldsymbol{R}$, $\widetilde{\omega}_{k-1} = \omega_{k-1}$, $\widetilde{\omega}_k = \omega_k$
2: $\boldsymbol{q}_{k-1} = \boldsymbol{q}_k + \boldsymbol{q}_{k-1}\, r_{k-1,k}\,, \quad \omega_{k-1} = \omega_k + \omega_{k-1} \|r_{k-1,k}\|^2$
3: $r_{k-1,k} = r_{k-1,k}^*\, \widetilde{\omega}_{k-1} / \omega_{k-1}$
4: $\boldsymbol{q}_k = \widetilde{\boldsymbol{q}}_{k-1} - \boldsymbol{q}_{k-1}\, r_{k-1,k}\,, \quad \omega_k = \widetilde{\omega}_{k-1} - \omega_{k-1} \|r_{k-1,k}\|^2$
5: **for** $l = k+1, \ldots, K$ **do**
6: $\quad r_{k-1,l} = r_{k-1,k}\, r_{k-1,l} + \widetilde{\omega}_k / \omega_{k-1}\, r_{k,l}$
7: $\quad r_{k,l} = \widetilde{r}_{k-1,l} - \widetilde{r}_{k-1,k}\, r_{k,l}$
8: **end for**
9: **for** $l = 1, \ldots, k-2$ **do**
10: $\quad r_{l,k-1} = r_{l,k}$
11: $\quad r_{l,k} = \widetilde{r}_{l,k-1}$
12: **end for**

If the Lovász condition is triggered (Line 17), the columns are swapped and the GSO has to be updated (UPDATE_QR).

4) Diversity Order: LRA LE has been proven to completely utilize the CV *MIMO receive diversity* $\Delta_{\mathrm{LRA,cv}} = L$ [16], [7]. Since in case of the QV channel (10) the number of random variables is doubled (cf. Sec. IV-A), LRA LE exploits the QV channel's receive diversity $2\,L$. In general, we have[7]

$$\Delta_{\mathrm{LRA}} = D_{\mathrm{ch}}/2 \cdot L\,, \tag{30}$$

i.e., a decrease of $L/2$, L, and $2\,L$ decades per $10\,\mathrm{dB}$ increase in SNR is present for RV, CV, and QV channels, respectively.

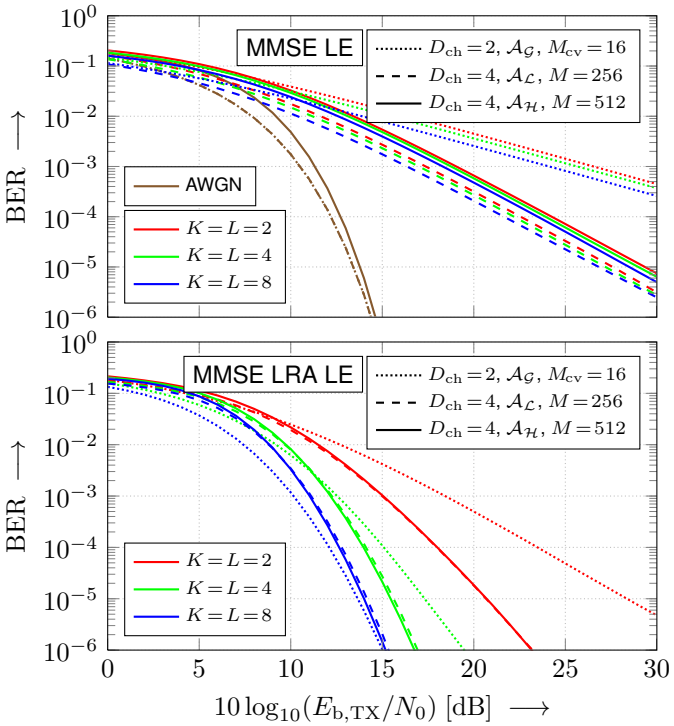

Fig. 5. Average BER over the SNR in dB in for CV ($D_{\mathrm{ch}} = 2$) and QV ($D_{\mathrm{ch}} = 4$) multi-user MIMO fading channels. Variation of MIMO dimensions $K = L$ and constellation $\mathcal{A}$. Top: Equalization via MMSE LE. For reference, results for the AWGN scenario are shown. Bottom: Equalization via MMSE LRA LE. CLLL for $D_{\mathrm{ch}} = 2$ and QLLL for $D_{\mathrm{ch}} = 4$, both with $\delta = 0.75$.

V. Numerical Results

In the following, we provide numerical results, particularly the average over 10^6 channel realizations and 10^3 symbols per channel. All variants of the LLL algorithm are applied with the standard parameter $\delta = 0.75$. Since we focus on the diversity behavior, we restrict to uncoded transmission.

Fig. 5 (Top) shows the bit error rate (BER) over the SNR. For reference, the CV and the QV AWGN channel are compared. The 16QAM constellation $\mathcal{A}_{\mathcal{G}}$ (CV; $D_{\mathrm{ch}} = 2$) and the 256-ary LI-based one $\mathcal{A}_{\mathcal{L}}$ (QV; $D_{\mathrm{ch}} = 4$), each with $M_{\mathrm{d}} = 4$, possess the same BER. Hence, the bandwidth efficiency is doubled while the power efficiency stays the same. The 512-ary HI-based constellation $\mathcal{A}_{\mathcal{H}}$ only leads to a slight decrease in performance, caused by the marginally higher variance σ_x^2 and the non-Gray labeling. Besides, the results for the multi-user MIMO fading channel and MMSE LE via (23) are given. Independently from the number of users/antennas, the diversity is determined by D_{ch}, i.e., $\Delta_{\mathrm{LE}} = 1$ for CV and $\Delta_{\mathrm{LE}} = 2$ for QV channels, cf. (24). In contrast, increasing the MIMO dimensions only results in a very small SNR gain.

In Fig. 5 (Bottom), MMSE LRA LE is applied to the multi-user fading scenario. To that end, the CLLL ($\mathcal{A}_{\mathcal{G}}$) and the QLLL ($\mathcal{A}_{\mathcal{L}}$, $\mathcal{A}_{\mathcal{H}}$) have been employed. We clearly see that the diversity is doubled by utilizing QV instead of CV channels as expected according to (30). We may, e.g., achieve $\Delta_{\mathrm{LRA}} = 4$ via $D_{\mathrm{ch}} = 2$ and $K = L = 4$, or alternatively by choosing $D_{\mathrm{ch}} = 4$ and $K = L = 2$. As for both $\mathcal{A}_{\mathcal{L}}$ and $\mathcal{A}_{\mathcal{H}}$

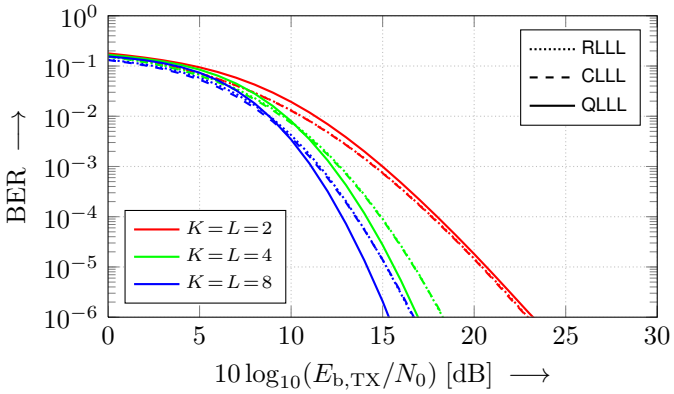

Fig. 6. Average BER over the SNR in dB for QV multi-user MIMO transmission ($D_{\mathrm{ch}}=4$) and the 256-ary LI-based constellation $\mathcal{A}_{\mathcal{L}}$. Variation of the MIMO dimensions $K=L$. RLLL reduction via (5), CLLL reduction via (4), and QLLL reduction, all of them with parameter $\delta=0.75$.

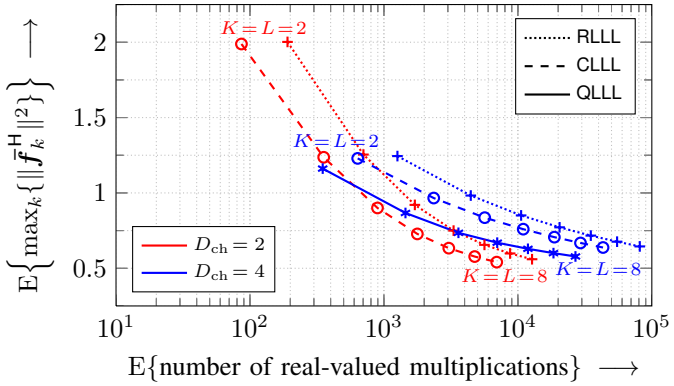

Fig. 7. Expectation of the maximum squared row norm of $\bar{\boldsymbol{F}}$ over the expectation of the required number of RV multiplications in the RLLL/CLLL/QLLL algorithm ($\delta=0.75$) for the CV ($D_{\mathrm{ch}}=2$) and QV ($D_{\mathrm{ch}}=4$) flat-fading MIMO channel. Variation of the MIMO dimensions $K=L$.

the quantization in the receiver has to be performed w.r.t. $\mathcal{H}$ (cf. Fig. 4), they nearly perform the same. If $K=L=8$, all curves are already close to the AWGN ones (Fig. 5 (Top)).

In Fig. 6, we restrict to QV channels ($D_{\mathrm{ch}}=4$), MMSE LRA LE, and the 256-ary constellation $\mathcal{A}_{\mathcal{L}}$. We compare the curves obtained by the QLLL (Fig. 5 (Bottom)) with the ones obtained via RLLL or CLLL (implemented by analogy with Algorithm 2), utilizing the RV or CV representations of the QV channel matrices according to (5) or (4), respectively. While all variants achieve full diversity, the QLLL additionally provides an SNR gain right up to 1 dB. It is caused by $\mathcal{Q}_{\mathcal{H}}\{\cdot\}$ in the size-reduction step: As $\mathcal{H}$ has the densest four-dimensional packing [1], the average quantization error is reduced in relation to the lattice $\mathbb{Z}^4$ (RLLL) or $\mathcal{G}^2$ (CLLL). In other words, the next lattice point may be located closer. Thus, the average noise enhancement of the remaining non-integer equalization via $\bar{\boldsymbol{F}}$ is lowered. We call this property the *factorization gain of the QLLL algorithm*.

In Fig. 7, the expectation of the maximum squared row norm of $\bar{\boldsymbol{F}}$ is depicted over the expected number of RV multiplications in the R/C/QLLL (computational complexity, cf. [4]), varying $K=L$. In the case of CV channels ($D_{\mathrm{ch}}=2$), RLLL (via RV representation) and CLLL nearly perform the same, but the CLLL lowers the complexity, cf. [7]. For QV channels ($D_{\mathrm{ch}}=4$), the same is valid when comparing RLLL and CLLL. In contrast, the QLLL not only lowers the complexity but also enables the abovementioned factorization gain.

VI. Summary and Conclusions

Multi-user MIMO equalization over QV arithmetic has been discussed. To this end, the transition to a CV transmission with dual-polarized antennas has been established. Given the QV channel model, the related diversity orders are doubled in comparison to the CV one. Besides, LLL reduction over quaternions (QLLL reduction) has been proposed utilizing the set of Hurwitz integers. It not only reduces the complexity in relation to RLLL or CLLL reduction, but additionally provides a factorization gain due to a denser packing of the lattice.

References

[1] J.H. Conway, N.J.A. Sloane. *Sphere Packings, Lattices and Groups*. Third Edition, Springer, 1999.

[2] J.H. Conway, D.A. Smith. *On Quaternions and Octonions: Their Geometry, Arithmetic, and Symmetry*. Taylor & Francis, 2003.

[3] Y.H. Cui, R.L. Li, H.Z. Fu. A Broadband Dual-Polarized Planar Antenna for 2G/3G/LTE Base Stations. *IEEE Trans. Antennas Propag.*, pp. 4836–4840, Sep. 2014.

[4] R.F.H. Fischer. Complexity-Performance Trade-Off Algorithms for Combined Lattice-Reduction and QR decomposition. *Int. J. of Electr. and Commun. (AEÜ)*, pp. 871–879, 2012.

[5] R.F.H. Fischer, M. Cyran, S. Stern. Factorization Approaches in Lattice-Reduction-Aided and Integer-Forcing Equalization. *Int. Zurich Seminar on Commun.*, pp. 108–112, Mar. 2016.

[6] R.F.H. Fischer, J.B. Huber, S. Stern, P.M. Guter. Multilevel Codes in Lattice-Reduction-Aided Equalization. *Int. Zurich Seminar on Commun.*, pp. 133–137, Feb. 2018.

[7] Y.H. Gan, C. Ling, W.H. Mow. Complex Lattice Reduction Algorithm for Low-Complexity Full-Diversity MIMO Detection. *IEEE Trans. Signal Process.*, pp. 2701–2710, July 2009.

[8] O.M. Isaeva, V.A. Sarytchev. Quaternion Presentations Polarization State. *2nd Topical Symp. on Combined Optical-Microwave Earth and Atmosphere Sensing*, pp. 195–196, Apr. 1995.

[9] M.Y. Li, *et al*. Eight-Port Orthogonally Dual-Polarized Antenna Array for 5G Smartphone Applications. *IEEE Trans. Antennas Propag.*, pp. 3820–3830, June 2016.

[10] W. Liu. Channel Equalization and Beamforming for Quaternion-Valued Wireless Communication Systems. *J. of the Franklin Institute*, pp. 8721–8733, Dec. 2017.

[11] R. Müller, B. Cakmak. Channel Modelling of MU-MIMO Systems by Quaternionic Free Probability. *Int. Symp. on Inf. Theory*, pp. 2656–2660, July 2012.

[12] H. Napias. A Generalization of the LLL-Algorithm over Euclidean Rings or Orders. *J. de Théorie des Nombres de Bordeaux*, pp. 387–396, 1996.

[13] J. Seberry, *et al*. The Theory of Quaternion Orthogonal Design. *IEEE Trans. Signal Process.*, pp. 256–265, Jan. 2008.

[14] S. Stern, R.F.H. Fischer. Optimal Factorization in Lattice-Reduction-Aided and Integer-Forcing Equalization. *Int. ITG Conf. on Commun., Systems and Coding*, pp. 68–71, Feb. 2017.

[15] C. Stierstorfer. *A Bit-Level-Based Approach to Coded Multicarrier Transmission*. Dissertation, University of Erlangen-Nuremberg, 2009.

[16] M. Taherzadeh, A. Mobasher, A.K. Khandani. LLL Reduction Achieves the Receive Diversity in MIMO Decoding. *IEEE Trans. Inf. Theory*, pp. 4801–4805, Dec. 2007.

[17] C. Windpassinger, R.F.H. Fischer. Low-Complexity Near-Maximum-Likelihood Detection and Precoding for MIMO Systems using Lattice Reduction. *IEEE Inf. Theory Workshop*, pp. 345–348, Mar. 2003.

[18] B.J. Wysocki, T.A. Wysocki, J. Seberry. Modeling Dual Polarization Wireless Fading Channels using Quaternions. *IST Workshop on Sensor Netw. and Symp. on Trends in Commun.*, pp. 68–71, June 2006.

[19] H. Yao, G.W. Wornell. Lattice-Reduction-Aided Detectors for MIMO Communication Systems. *IEEE Gl. Telecom. Conf.*, Nov. 2002.